Tactile chemomechanical transduction based on an elastic microstructured array to enhance the sensitivity of portable biosensors

Wang, Ting; Qi, Dianpeng; Yang, Hui; Liu, Zhiyuan; Wang, Ming; Leow, Wan Ru; Chen, Geng; Yu, Jiancan; He, Ke; Cheng, Hongwei; Wu, Yun-Long; Zhang, Han; Chen, Xiaodong

2018

Wang, T., Qi, D., Yang, H., Liu, Z., Wang, M., Leow, W. R., . . . Chen, X. (2019). Tactile chemomechanical transduction based on an elastic microstructured array to enhance the sensitivity of portable biosensors. Advanced Materials, 31(1), 1803883-. doi:10.1002/adma.201803883

https://hdl.handle.net/10356/137812

https://doi.org/10.1002/adma.201803883

DOI: 10.1002/((please add manuscript number))
Article type: Communication

Tactile Chemomechanical Transduction Based on Elastic Microstructured Array to Enhance the Sensitivity of Portable Biosensors

Ting Wang, Dianpeng Qi, Hui Yang, Zhiyuan Liu, Ming Wang, Wan Ru Leow, Geng Chen, Jiancan Yu, Ke He, Hongwei Cheng, Yun-Long Wu, Han Zhang, and Xiaodong Chen**

Dr. T. Wang, Prof. H. Zhang
International Collaborative Laboratory of 2D Materials for Optoelectronics Science and Technology of Ministry of Education, Shenzhen Engineering Laboratory of Phosphorene and Optoelectronics, College of Optoelectronic Engineering, Shenzhen University, 3688 Nanhai Avenue, Shenzhen, Guangdong, China
E-mail: hzhang@szu.edu.cn

Dr. T. Wang, Dr. D. Qi, Dr. H. Yang, Dr. Z. Liu, Dr. M. Wang, Dr. W. R. Leow, G. Chen, Dr. J. Yu, Dr. K. He, Prof. X. Chen
Innovative Center for Flexible Devices (iFLEX), School of Materials Science and Engineering, Nanyang Technological University, 50 Nanyang Avenue, 639798, Singapore
E-mail: chenxd@ntu.edu.sg

H. Chen, Prof. Y.-L. Wu
Fujian Provincial Key Laboratory of Innovative Drug Target Research and State Key Laboratory of Cellular Stress Biology, School of Pharmaceutical Sciences, Xiamen University, Xiamen 361102, P. R. China

Keywords: tactile sensor, chemomechanical transduction, healthcare, microstructured array, signal amplification

Tactile sensors capable of perceiving biophysical signals such as force, pressure, or strain have attracted extensive interests for versatile applications in electronic skin, non-invasive health care, and biomimetic prostheses. Despite these great achievements, they are yet incapable of detecting bio/chemical signals which provide even more meaningful and precise health information, due to the lack of efficient transduction principles. Herein, we propose a tactile chemomechanical transduction strategy that enables the tactile sensor to perceive bio/chemical signals. In this methodology, pyramidal tactile sensors were linked with biomarker-induced gas-producing reactions, which would transduce biomarker signals to electrical signals in real time. The method is advantageous as it enhances electrical signals by

more than 10 fold based on a triple-step signal amplification strategy, as compared to traditional electrical biosensors. It also constitutes a portable and general platform capable of quantifying a wide spectrum of targets including carcinoembryonic antigen, interferon-γ, and adenosine. Such tactile chemomechanical transduction would greatly broaden the application of tactile sensors toward bio/chemical signals perception which can be used in ultrasensitive portable biosensors and chemical-responsive chemomechanical systems.

Tactile sensor converts the force information of an object or event to electrical signals based on piezoresistivity, capacitance, and piezoelectricity principles.[1-3] Recent years have witnessed the booming development of tactile sensors with excellent mechanical adaptability and ultrasensitivity, which have been succesfully applied in electronic skin to "feel" irritants (several Pa), non-invasive healthcare to record pulse waves (low-pressure <10 kPa), and biomimetic prostheses to perceive vibrations.[4-6] Currently, the application of these tactile sensors are limited to the detection of physical signals such as pressure, lateral strain and vibration.[7-10] Due to the lack of efficient transduction principles, tactile sensors are yet incapable of perceiving biochemical signals. As these biochemical signals such as proteins and metabolites are widely existed and contain even more valuable and precise health information at the molecular level,[11] the detection of biomarkers by tactile sensors may significantly broaden their application in ultrasensitive portable biosensors and chemical-responsive chemomechanical systems. Therefore, the key aim of our research is to develop a tactile chemomechanical transduction methodology that transduce biomarkers information to force or pressure signals detectable by tactile sensors, which could endow well-developed tactile sensors with the capability of perceiving biochemical signals (**Figure 1**a, b).

Bio/chemomechanical coupling is a common and important mechanism for precise self-regulation in biological organisms, such as the opening of the protein channel in response to chemical stimli.[12-15] However, it is challenging to utilize this natural coupling effect for

portable biosensing.[16-18] The main challenges are (i) the difficulty to detect the weak mechanical signals of nano- or micro- scale in real time and *in-situ* without bulky detection instruments, and (ii) the lack of quantitative correlationship between mechanical signals and biomarkers.[19-20] To solve the intractable problem regarding weak mechanical signal detection, we propose tactile sensors based on elastic microstructured array, which possess the advantageous features of ultrasensitivity, real-time monitoring, and ready integration with electronics. Meanwhile, it is noted that many chemical reactions have close and mutual interaction with environment pressure, especially for reactions containing liquid-gas phase transition.[21-23] Hence, by rationally linking the biomarkers with a gas-producing reaction using nanocatalysts labeled to biomolecules as the bridge, we build a correlation between biomarker and pressure. In this way, tactile chemomechanial transduction is designed, in which tactile sensors are utilized to sensitively perceive biomarker-induced mechanical signals.

The design comprises of a biomarker-induced gas-producing reaction and a microstructured tactile sensor (Figure 1c). The bioreaction is based on a nanocatalyst-labeled sandwhich immunocomplex, which trigger gas-producing reactions by the specific recognition of biomarkers. An elastomer film comprising a pyramidal array is selected as the deformation layer, due to the inherently elastic feature of elastomers and the small shape factor of pyramids.[9] The rationale is that pyramidal tactile sensors can transduce biomarker-induced pressure signals to electrical signals which quantitatively reflect biomarker information. Compared to traditional electrochemical biosensors that rely on electron transfer between electrodes and active species in solution, our methodology is characterized by the following advantages: i) providing a general method to readily transfer electro-inert reactions into electrical signals; ii) avoiding direct contact between the electrode and the solution, which excludes the electrode poisoning phenomena and modification procedures; iii) introducing a triple-step signal amplification that includes catalytic effect, gas-producing

reactions, and elastic pyramidal array which can enhance electrical signals by more than 10 fold compared to traditional electrical biosensors. Based on the aforementioned advantages, tactile biosensors are portable, sensitive, and general for a wide spectrum of targets including carcinoembryonic antigen (CEA), interferon-γ (IFN-γ), and adenosine. Hence, the tactile chemomechanical transduction methodology, which allows soft tactile sensors to perceive biomarkers, which would be extremely valuable in portable diagnostics as well as constructing responsive multimodal chemomechanical systems.

The fabrication of the tactile biosensor includes the preparation of device framework and integration of pyramidal tactile sensors. The framework was firstly designed via Solidworks software and fabricated using the UV-assisted three dimention (3D) printing method. Each of device contains a chamber with inner volumn of 0.8 mL and two square channels of 2 × 2 mm (Figure 1d). One channel serves as the connection to tactile sensors and the other one as the liquid inlet/outlet. Tactile sensor has three components, the pyramidal polydimethylsiloxane (PDMS) film, CNT conductive layer, and interdigital counter electrode. PDMS film with uniform pyramid diameter of 6 μm was firstly prepared via curing PDMS precursor on the pyramidal Si template (Figure S1a, Supporting Information).[9, 24] Pyramid is chosen here because of the optimal geometrical shape with the high deformation ability upon compression due to the strain concentration.[25] After O_2 treatment on the designed pattern (2 × 2 mm) of PDMS film, carbon nanotube solution was dropped on the patterned area. CNT network with high stability was selected here and attached on the pyramidal PDMS layer based on hydrogen bond between carboxylated carbon tubes and hydroxyl functionalized PDMS film (Figure S1b, Supporting Information).[26] CNT/PDMS film was then pasted on the device using semi-cured PDMS as the glue. Interdigital Au/Cr pattern with width and gap of 200 μm on polyethylene terephthalate (PET) substrate was used as the counter electrodes for convenient circuit connection (Figure S1c, Supporting Information). Au/Cr electrode was then fixed above the pyramidal film by glass and the epoxy glue. Glass keeps the flatness of

counter electrode and the glue avoids the position shift of electrodes upon pressure. In this way, a fully integrated chemomechanial transduction device was fabricated via integrating pyramidal CNT/PDMS film and interdigital counter electrode on 3D-printed framework. Details of the device fabrication are given in the Supporting Information.

The performance of tactile sensor was firstly characterized with a constant voltage of 1 V. Pyramidal CNT/PDMS film illustrates a linear detection range from 120 to 2400 Pa with a sensitivity of 0.15 Pa^{-1} (**Figure 2**a and S1d, Supporting Information). Excellent stability of the sensor is demonstrated by performance variation of 5.46% during repeatedly applying and removing pressure for 5000 cycles (Figure 2b). Response time of tactile sensor is measured to be 250 μs by monitoring the voltage drop of a 50 Ω resistor in series with the tactile sensor (Figure 2c). Compared to previous piezoresistive pressure sensors,[9, 27-31] pyramidal CNT/PDMS sensor shows high sensitivity and rapid response (Table S1). These features are advantageous for the sensitive, reliable and real-time transduction of pressure signals of gas-producing reactions.

The gas-producing reaction is based on the catalytic decomposition of H_2O_2 which is efficient, environmental benign, and catalyst-dependent. To obtain a high efficient system, a series of catalysts[32-37] were investigated included natural horseradish peroxidase (HRP), platium nanoparticles (Pt NPs), Prussian blue nanoparticles (PB NPs), and MnO_2 NPs. Procedures include adding H_2O_2 solution and catalyst in chamber through the channel, sealing the device and then recording the current at a constant voltage of 1 V. With the gas production in the chamber, the pressure inside is enhanced, which results in the pressing of the conductive pyramid onto the counter electrode. Then the contact area between the film and electrode increases, which causes the device to experience a decrease in resistance and thus an increase in current until reaching the maximal deformation of pyramid. Hence, the current changes reflect the information of gas-producing reactions like catalytic efficiency and the amount of catalysts.

It is noted that the current increment varies for different catalysts and ascends following the sequence of MnO_2 NPs, PB NPs, HRP, and Pt NPs (Figure 2d). Within the same reaction interval, the larger amount of current increment indicates a higher gas-producing rate corresponding to a higher catalytic efficiency. The efficiency of catalysts was quantified via kinetic parameters of catalysts (k_{cat}) based on steady-state kinetics. We obtain the k_{cat} value for Pt NPs of 5.20×10^3 s^{-1} which is larger than that of HRP (1.72×10^3 s^{-1}), PB NPs (2.46×10^2 s^{-1}) and MnO_2 (1.89×10^2 s^{-1}) (Figure S2 and Table S2, Supporting Information), and they are comparable to literatures.[32, 35] Hence, tactile chemical sensor provides an avenue to quantify the catalytic efficiency and Pt NPs with highest efficiency are selected as the optimal biolabels.

Then, the quantitative detection of the concentration of Pt NPs was tested. Considering the maximal deformation of pyramidal elastomer, current change ($\Delta i/i_0$) at 600 s is used as the quantitative parameter where Δi is the current change at a reaction time interval of 600 s, and i_0 is the initial current. The sensitivity for Pt NPs ($S_{Pt\ NPs}$) of tactile sensors is defined as $\delta(\Delta i/i_0)/\delta c_{Pt\ NPs}$. The results show that $\Delta i/i_0$ is proportional to the concentration of Pt NPs, indicating that the tactile sensor could quantitatively read out the concentration of Pt NPs, which is a prerequisite for Pt NPs-labeled biomarker detection (Figure 2e).

As the signals are dependent on the deformation of elastomer, Young's modulus of PDMS is expected to affect the sensing performance. To figure out the optimal property of elastomer, PDMS with Young's modulus of 1.31, 0.69, and 0.28 MPa were prepared and denoted as $PDMS_{10}$, $PDMS_{15}$, and $PDMS_{20}$, respectively (Figure S3d, Supporting Information). $PDMS_{20}$ based device showed $S_{Pt\ NPs}$ of 447 nM^{-1} and linear detection range (LDR) from 0.001 to 0.6 nM, compared with $PDMS_{15}$ ($S_{Pt\ NPs}$: 261 nM^{-1}; LDR: 0.005~1 nM), and $PDMS_{10}$ ($S_{Pt\ NPs}$: 119 nM^{-1}; LDR: 0.01~2.5 nM) (Figure 2e and Figure S3a-c, Supporting Information). PDMS with smaller Young's modulus experiences a larger deformation upon a certain pressure and exhibits higher sensitivity which is desirable for trace biomarker detection in early diagnosis

of diseases. Comparatively, PDMS with larger Young's modulus shows wider detection ranges, which is advantageous for precise detection of biomarkers with broad concentration distributions. In our case, $PDMS_{20}$ was used for tactile biosensors to achieve a highly sensitive portable bioassay platform.

Moreover, the robustness of tactile chemical sensor were evaluated by the device to device variations. Based on the performance of five different devices, the variation of individual catalytic system is less than 9.1% indicating the robustness of device fabrication process (Figure S4, Supporting Information). The good reliability and stability of tactile chemical sensor was verified by using one device to repeatedly monitor the reaction. For every test, the procedures are the same which includes injecting newly-prepared solution, sealing, recording the current, and then unsealing. The pressure can be reset by unsealing the chamber manually within seconds. The reactants including biomaterials are stored at 4 ^{o}C before use and they are disposed after one test. The concentration of H_2O_2 and Pt NPs were kept unchanged, which are 1 M, and 600 pM, respectively. The current of sensor showed repeated gradual increase and shape decrease which were due to the gas-producing reactions in chamber and pressure reset operation, respectively, as shown in Figure 2f. A cyclic testing of 50 cycles shows variation less than 7.31% which illustrated the good reliability and stability of device (Figure S5, Supporting Information). For comparison, we also tested tactile biosensors based on unstructured elastomer. It is clearly to see that the current could not return to the original state when the chamber was unsealing (Figure S6, Supporting Information). This might be ascribed to that the unstructured elastomer stuck to the electrode due to the visco-elastic property of elastomer. In contrast, pyramid structure acts as space to enable the elastic deformation of microstructure, which minimizes the problems associated with visco-elastic behaviour of elastomer.[1] Consequently, based on chemomechanical transduction principle, pyramidal tactile chemical sensors realize the stable, robust, real-time, and *in-situ* perception of the chemical signals.

Utilizing Pt NPs as the labels to biomolecules, tactile biosensors are constructed based on elastic pyramidal arrays to perceive biomarkers, which provide a sensitive and stable platform for portable biosensors. Portable devices will be more and more important in furture medical system as they provide a convenient way to alert patients to perceive the abnormality of biomarkers in advance and take precautions before the deterioration of diseases. Considering that the development and spread of cancer is a mutistep process, portable cancer diagnostics should be even more meaningful as early diagnosis of cancer greatly increases the treatment efficiency. Hence, CEA, which is a model cancer biomarker, was chosen as the detection target to demonstrate tactile biosensors.

To achieve tactile biosensors for CEA, the device was linked with a specific immuno-reaction (**Figure 3**). Details are given in the Supporting Information. Briefly, core shell Fe_3O_4@SiO_2/Au/antibody 1 (Ab1) were firstly synthesized to specifically capture the antigen (Figure S7, Supporting Information).[38-40] Antibody 2 (Ab2) was labeled with Pt NPs using *in-situ* polymerization with dopamine as the monomer.[34] With the presence of CEA, a sandwich immunocomplex is formed based on the specific interaction between antibody and CEA, which is similar to the sandwich immunoassay. Based on immunoreaction followed by magnetic separation and rinsing to remove the unanchored or physical adsorbed Pt NPs, magnetic Ab1/CEA/Pt NPs-Ab2 was achieved (Figure 3a and S8, Supporting Information). After dissociation of the magnetic composites, bioreaction suspensions that contain Pt NPs were added into the chamber for detection. The current gradually increases (Figure 3b) which suggests the successful capture of Pt NPs by specific immunoreaction. When increasing the concentrations of CEA in the bioreactions, the current increases more quickly and reaches a higher platform. It is reasonable that more CEA anchor more amount of Ab2/Pt NPs and thus induce higher decompostion rate of H_2O_2 corresponding to larger amount of current increment. This correlationship enables the quantitative detection of biomarkers. Based on current changes ($\Delta i/i_0$), tactile biosensors show LDR from 0.05 to 50 ng/mL for CEA (Figure 3c).

The detection range fully covers the range of CEA concentration in serum from healthy (≤ ~ 2.5 ng/mL) and patient (tumors ≤ ~ 20 ng/mL and potential tumor metastasis ≥ ~ 20 ng/mL).[41-42]

Good anti-inference was verified by negligible current changes upon the addition of other tested species in the bioreactions (**Figure 4**a) including glucose, HSA, dopamine, adenosine, and IFN-γ which might be present in serum. The reliability of tactile biosensors was proved by the satisfactory recoveries (variation less than 4.16%) in real serum spiked with CEA (Figure 4c). Noted that Furthermore, we tested clinic serum samples which are from one healthy people, one patient with benign tumors and five cancer patients. It is found that the $\Delta i/i_0$ value was positively correlated with CEA concentration measured by classical Elisa assay. Not only that, the CEA concentration obtained from tactile biosensor also reflects the disease status of patients which could be utilized for predicting the disease status, including health, benign tumor, and potential tumor metastasis (Figure 4b).[41-42]

As Pt NPs is a kind of general biolabels, the generality of tactile biosensor was further testified via IFN-γ and adenosine. The formal is a cytokine related to many infectious diseases and the latter is an important biological cofactor.[43] We show that tactile biosensors successfully detect IFN-γ from 0.5 to 25 nM and adenosine from 5 to 60 μM through choosing specific recognition biomolecules (Figure 3c, S9a-c, Supporting Information). These range are of clinic significance to monitor the physiological levels of the cytokine secreted by the immune cells (nanomolar range),[44-45] and abnormality of adenosine in urine (tens of micromolar) due to kidney function.[46-47] Further interference experiment showed that potential interference species caused variations within 8.3%, and 8.8%, respectively, for IFN-γ, and adenosine (Figure S9d and e, Supporting Information). The good anti-interference ability is ascribed to the specific binding ability of aptamer.

Moreover, when tactile biosensors are combined with wireless Ammeter, current signals can be transmitted to smartphone for portable biosensors (Figure 4e and f). The Keithley was also used to collect the data for comparison (Figure S10). The consistency of results on smartphone with that on Keithley indicated the reliability of portable device based on wireless technology. Compared with previous commercial pressure meter-based biosensors, the tactile biosensor shows advantages in terms of miniaturization and integration which can be facile connected with well-developed electronics (Table S3). The customized sensor arrays by 3D-printing technology will also benifit high throughput detection. For practical application, the overall operation for user part is sufficiently simple using biomolecules prepared in advance. The H_2O_2 solution is kept in the chamber which will not contact with or cause any harm to biosubstance during biosensing process. Any inexperienced users can be trained in a few minutes, including mixing biomolecules, magnetic separation, and device testing. The testing time could be further reduced via increasing the Pt NPs loading amount, enhancing immune recognition efficiency, and chamber design with reduced volume of space. Hence, tactile biosensors provide a reliable, general and portable platform for disease diagnostics.

Compared with previous electrical transducers for CEA including electrochemical, photoelectrical, and electrical-resistance biosensors, tactile biosensor shows advantages in terms of sensitivity, generality and portability. Figure 4d illustrates the performance of biosensors based on catalytic current,[48-53] redox current of labeled species,[54-56] photo-activated current,[57-59] and electrochemical resistance,[60-65] respectively. The sensitivity was calculated based on $\Delta i/i_0$ per unit concentration of CEA (ng/mL) on unit area of electrode (cm^2). These biosensors generally show current signals at nano- or microampero scale and sensitivity with mean value less than 30 due to the limitation of electrode area, activity and concentrations of electroactive species. Comparatively, the tactile biosensor transfers reactions into electrical signals at miliampero scale via a peizoresistive principle and shows sensitivity with value of 372. We also quantitatively described the operation of each step

based on reaction efficiency, stoichiometric principles, and ideal gas law (details given in the Supporting Information). CEA-induced pressure (Pa) is linearly dependent on the concentration of CEA (ng/mL) with a fitted expression of $P = 144.85c_{CEA} + 6.41$ (Figure S11). Based on sensing performance of tactile sensor, the estimated value of sensitivity is 553.33 ± 80, which is comparable to our experiment data. The sensitivity of tactile biosensor is 10-fold higher than traditional electrochemical biosensors that generally contain one-step amplification such as catalytic effects. Tactile biosensors contain triple-step signal-amplification which is responsible for the high sensitivity. They are (i) liquid-gas phase transition with pressure expanding by 2–3 orders of magnitude, (ii) Pt NPs work as catalyst which enables one molecular bio-recognition event to generate more than one million O_2 molecules, (iii) pyramidal PDMS films sensitively transfer small pressure to milliampero current signals. Meanwhile, triple-step signal-amplification readily enables the transduction of non-redox reactions such as biomolecular recognition reactions into amplified electrical signals. Moreover, this transduction methodology is non-invasive where the electrode did not contact with the solution. This feature avoids electrode modification and eliminates the poisoning effect of electrode, which leads to better reproducibility and stability of tactile biosensors.

In summary, we demonstrated a tactile chemomechanical transduction that allows tactile sensor to preceive bio/chemical signals which provide a biosensing platform with high sensitivity, wide generality, and portability. The principle is that based on elastic pyramidal array, tactile sensors transduce the signals of biomarker-induced gas-producing reactions to electrical signals via a real-time and senstive way. Through selecting optimal biorecognition molecules, we show that tactile sensors realize the quantification of a variety of targets including CEA, IFN-γ, and adenosine. Moreover, this platform is portable and readily to be integrated with wireless technologies for constructing portable diagnostic devices. We expect that the concept of tactile chemomechanical transduction greatly broadens the application

range of tactile sensors and has the potential to build up a multimodal device capable of monitoring chemical, electrophysiological and physical signal.

Supporting Information

Supporting Information is available from the Wiley Online Library or from the author.

Acknowledgements

We thank the financial support from the National Research Foundation (NRF), Prime Minister's office, Singapore, under its NRF Investigatorship (NRF2016NRF-NRF1001-21), Singapore Ministry of Education (MOE2014-T2-2-140), NTU-Northwestern Institute for Nanomedicine, K. C. Wong Education Foundation, and China Postdoctoral Science Foundation Funded Project (2016M592518).

References

[1] S. C. Mannsfeld, B. C. Tee, R. M. Stoltenberg, C. V. H. Chen, S. Barman, B. V. Muir, A. N. Sokolov, C. Reese, Z. Bao, *Nat. Mater.* **2010**, *9*, 859.

[2] G. Y. Bae, S. W. Pak, D. Kim, G. Lee, D. H. Kim, Y. Chung, K. Cho, *Adv. Mater.* **2016**, *28*, 5300.

[3] S. Gong, W. Schwalb, Y. Wang, Y. Chen, Y. Tang, J. Si, B. Shirinzadeh, W. Cheng, *Nat. Commun.* **2014**, *5*, 3132.

[4] Y. Liu, K. He, G. Chen, W. R. Leow, X. Chen, *Chem. Rev.* **2017**, *117*, 12893.

[5] Y. Zang, F. Zhang, C.-a. Di, D. Zhu, *Mater. Horiz.* **2015**, *2*, 140.

[6] Y. Pang, K. Zhang, Z. Yang, S. Jiang, Z. Ju, Y. Li, X. Wang, D. Wang, M. Jian, Y. Zhang, *ACS Nano* **2018**, *12*, 2346.

[7] C. Pang, G.-Y. Lee, T.-i. Kim, S. M. Kim, H. N. Kim, S.-H. Ahn, K.-Y. Suh, *Nat. Mater.* **2012**, *11*, 795.

[8] D. J. Lipomi, M. Vosgueritchian, B. C. Tee, S. L. Hellstrom, J. A. Lee, C. H. Fox, Z. Bao, *Nat. Nanotechnol.* **2011**, *6*, 788.

[9] B. Zhu, Z. Niu, H. Wang, W. R. Leow, H. Wang, Y. Li, L. Zheng, J. Wei, F. Huo, X. Chen, *Small* **2014**, *10*, 3625.

[10] T. Wang, H. Yang, D. Qi, Z. Liu, P. Cai, H. Zhang, X. Chen, *Small* **2018**, *14*, 1702933.

[11] L. Wu, X. Qu, *Chem. Soc. Rev.* **2015**, *44*, 2963.

[12] L. Liu, Z. You, H. Yu, L. Zhou, H. Zhao, X. Yan, D. Li, B. Wang, L. Zhu, Y. Xu, *Nat. Mater.* **2017**, *16*, 1252.

[13] S. Kasas, F. S. Ruggeri, C. Benadiba, C. Maillard, P. Stupar, H. Tournu, G. Dietler, G. Longo, *Proc. Natl. Acad. Sci. U. S. A.* **2015**, *112*, 378.

[14] P. Cai, M. Layani, W. R. Leow, S. Amini, Z. Liu, D. Qi, B. Hu, Y. L. Wu, A. Miserez, S. Magdassi, X. Chen *Adv. Mater.* **2016**, *28*, 3102.

[15] L. D. Zarzar, J. Aizenberg, *Acc. Chem. Res.* **2014**, *47*, 530.

[16] X. He, M. Aizenberg, O. Kuksenok, L. D. Zarzar, A. Shastri, A. C. Balazs, J. Aizenberg, *Nature* **2012**, *487*, 214.

[17] J. Arlett, E. Myers, M. Roukes, *Nat. Nanotechnol.* **2011**, *6*, 203.

[18] P. M. Kosaka, V. Pini, J. Ruz, R. da Silva, M. González, D. Ramos, M. Calleja, J. Tamayo, *Nat. Nanotechnol.* **2014**, *9*, 1047.

[19] A. R. Studart, *Angew. Chem. Int. Ed.* **2015**, *54*, 3400.

[20] G. Longo, L. Alonso-Sarduy, L. M. Rio, A. Bizzini, A. Trampuz, J. Notz, G. Dietler, S. Kasas, *Nat. Nanotechnol.* **2013**, *8*, 522.

[21] A. Shastri, L. M. McGregor, Y. Liu, V. Harris, H. Nan, M. Mujica, Y. Vasquez, A. Bhattacharya, Y. Ma, M. Aizenberg, *Nat. Chem.* **2015**, *7*, 447.

[22] J. D. Besant, J. Das, I. B. Burgess, W. Liu, E. H. Sargent, S. O. Kelley, *Nat. Commun.* **2015**, *6*, 6978.

[23] Z. Zhu, Z. Guan, D. Liu, S. Jia, J. Li, Z. Lei, S. Lin, T. Ji, Z. Tian, C. J. Yang, *Angew. Chem. Int. Ed.* **2015**, *54*, 10448.

[24] D. Qi, L. Zheng, X. Cao, Y. Jiang, H. Xu, Y. Zhang, B. Yang, Y. Sun, H. H. Hng, N. Lu, L. Chi, X. Chen *Nanoscale* **2013**, *5*, 12383.

[25] B. C. K. Tee, A. Chortos, R. R. Dunn, G. Schwartz, E. Eason, Z. Bao, *Adv. Funct. Mater.* **2014**, *24*, 5427.

[26] Z. Liu, D. Qi, P. Guo, Y. Liu, B. Zhu, H. Yang, Y. Liu, B. Li, C. Zhang, J. Yu, B. Liedberg, X. Chen *Adv. Mater.* **2015**, *27*, 6230.

[27] C. Yeom, K. Chen, D. Kiriya, Z. Yu, G. Cho, A. Javey, *Adv. Mater.* **2015**, *27*, 1561.

[28] L. Pan, A. Chortos, G. Yu, Y. Wang, S. Isaacson, R. Allen, Y. Shi, R. Dauskardt, Z. Bao, *Nat. Commun.* **2014**, *5*, 3002.

[29] C. Hou, H. Wang, Q. Zhang, Y. Li, M. Zhu, *Adv. Mater.* **2014**, *26*, 5018.

[30] B. Su, S. Gong, Z. Ma, L. W. Yap, W. Cheng, *Small* **2015**, *11*, 1886.

[31] X. Wang, Y. Gu, Z. Xiong, Z. Cui, T. Zhang, *Adv. Mater.* **2014**, *26*, 1336.

[32] L. Gao, J. Zhuang, L. Nie, J. Zhang, Y. Zhang, N. Gu, T. Wang, J. Feng, D. Yang, S. Perrett, *Nat. Nanotechnol.* **2007**, *2*, 577.

[33] T. Wang, Y. Fu, L. Bu, C. Qin, Y. Meng, C. Chen, M. Ma, Q. Xie, S. Yao, *J. Phys. Chem. C* **2012**, *116*, 20908.

[34] Y. Fu, P. Li, T. Wang, L. Bu, Q. Xie, X. Xu, L. Lei, C. Zou, J. Chen, S. Yao, *Biosens. Bioelectron.* **2010**, *25*, 1699.

[35] T. Wang, Y. Fu, L. Chai, L. Chao, L. Bu, Y. Meng, C. Chen, M. Ma, Q. Xie, S. Yao, *Chem. Eur. J.* **2014**, *20*, 2623.

[36] M. Huang, Y. Jin, H. Jiang, X. Sun, H. Chen, B. Liu, E. Wang, S. Dong, *J. Phys. Chem. B* **2005**, *109*, 15264.

[37] T. Uemura, S. Kitagawa, *J. Am. Chem. Soc.* **2003**, *125*, 7814.

[38] T. Wang, L. Zhang, C. Li, W. Yang, T. Song, C. Tang, Y. Meng, S. Dai, H. Wang, L. Chai, *Environ. Sci. Technol.* **2015**, *49*, 5654.

[39] T. Wang, L. Zhang, H. Wang, W. Yang, Y. Fu, W. Zhou, W. Yu, K. Xiang, Z. Su, S. Dai, *ACS Appl. Mater. Interfaces* **2013**, *5*, 12449.

[40] Y. Deng, Y. Cai, Z. Sun, J. Liu, C. Liu, J. Wei, W. Li, C. Liu, Y. Wang, D. Zhao, *J. Am. Chem. Soc.* **2010**, *132*, 8466.

[41] D. Thomson, J. Krupey, S. Freedman, P. Gold, *Proc. Natl. Acad. Sci. U. S. A.* **1969**, *64*, 161.

[42] W. M. Steinberg, R. Gelfand, K. K. Anderson, J. Glenn, S. H. Kurtzman, W. F. Sindelar, P. P. Toskes, *Gastroenterology* **1986**, *90*, 343.

[43] Y. Xiang, Y. Lu, *Nat. Chem.* **2011**, *3*, 697.

[44] N. Tuleuova, C. N. Jones, J. Yan, E. Ramanculov, Y. Yokobayashi, A. Revzin, *Anal. Chem.* **2010**, *82*, 1851.

[45] S. Farid, X. Meshik, M. Choi, S. Mukherjee, Y. Lan, D. Parikh, S. Poduri, U. Baterdene, C.-E. Huang, Y. Y. Wang, *Biosens. Bioelectron.* **2015**, *71*, 294.

[46] H. Liu, Y. Xiang, Y. Lu, R. M. Crooks, *Angew. Chem. Int. Ed.* **2012**, *124*, 7031.

[47] V. Vallon, B. Muhlbauer, H. Osswald, *Physiol. Rev.* **2006**, *86*, 901.

[48] D. Feng, L. Li, X. Fang, X. Han, Y. Zhang, *Electrochim. Acta* **2014**, *127*, 334.

[49] D. Tang, J. Ren, *Anal. Chem.* **2008**, *80*, 8064.

[50] B. Su, J. Tang, H. Yang, G. Chen, J. Huang, D. Tang, *Electroanalysis* **2011**, *23*, 832.

[51] G. Sun, J. Lu, S. Ge, X. Song, J. Yu, M. Yan, J. Huang, *Anal. Chim. Acta* **2013**, *775*, 85.

[52] Z. Zhong, W. Wu, D. Wang, D. Wang, J. Shan, Y. Qing, Z. Zhang, *Biosens. Bioelectron.* **2010**, *25*, 2379.

[53] J. Gao, Z. Guo, F. Su, L. Gao, X. Pang, W. Cao, B. Du, Q. Wei, *Biosens. Bioelectron.* **2015**, *63*, 465.

[54] C. Ma, H. Liu, L. Zhang, H. Li, M. Yan, X. Song, J. Yu, *Biosens. Bioelectron.* **2018**, *99*, 8.

[55] J. Huang, J. Tian, Y. Zhao, S. Zhao, *Sens. Actuators, B* **2015**, *206*, 570.

[56] D. Lin, J. Wu, H. Ju, F. Yan, *Biosens. Bioelectron.* **2014**, *52*, 153.

[57] J. Wang, J. Long, Z. Liu, W. Wu, C. Hu, *Biosens. Bioelectron.* **2017**, *91*, 53.

[58] H. Yang, G. Sun, L. Zhang, Y. Zhang, X. Song, J. Yu, S. Ge, *Sens. Actuators, B* **2016**, *234*, 658.

[59] S. Ge, W. Li, M. Yan, X. Song, J. Yu, *J. Mater. Chem. B* **2015**, *3*, 2426.

[60] Y. Wang, H. Xu, J. Luo, J. Liu, L. Wang, Y. Fan, S. Yan, Y. Yang, X. Cai, *Biosens. Bioelectron.* **2016**, *83*, 319.

[61] X. Cai, S. Weng, R. Guo, L. Lin, W. Chen, Z. Zheng, Z. Huang, X. Lin, *Biosens. Bioelectron.* **2016**, *81*, 173.

[62] J. Liu, J. Wang, T. Wang, D. Li, F. Xi, J. Wang, E. Wang, *Biosens. Bioelectron.* **2015**, *65*, 281.

[63] L. Zhu, L. Xu, N. Jia, B. Huang, L. Tan, S. Yang, S. Yao, *Talanta* **2013**, *116*, 809.

[64] H. Quan, C. Zuo, T. Li, Y. Liu, M. Li, M. Zhong, Y. Zhang, H. Qi, M. Yang, *Electrochim. Acta* **2015**, *176*, 893.

[65] N. Liu, X. Chen, Z. Ma, *Biosens. Bioelectron.* **2013**, *48*, 33.

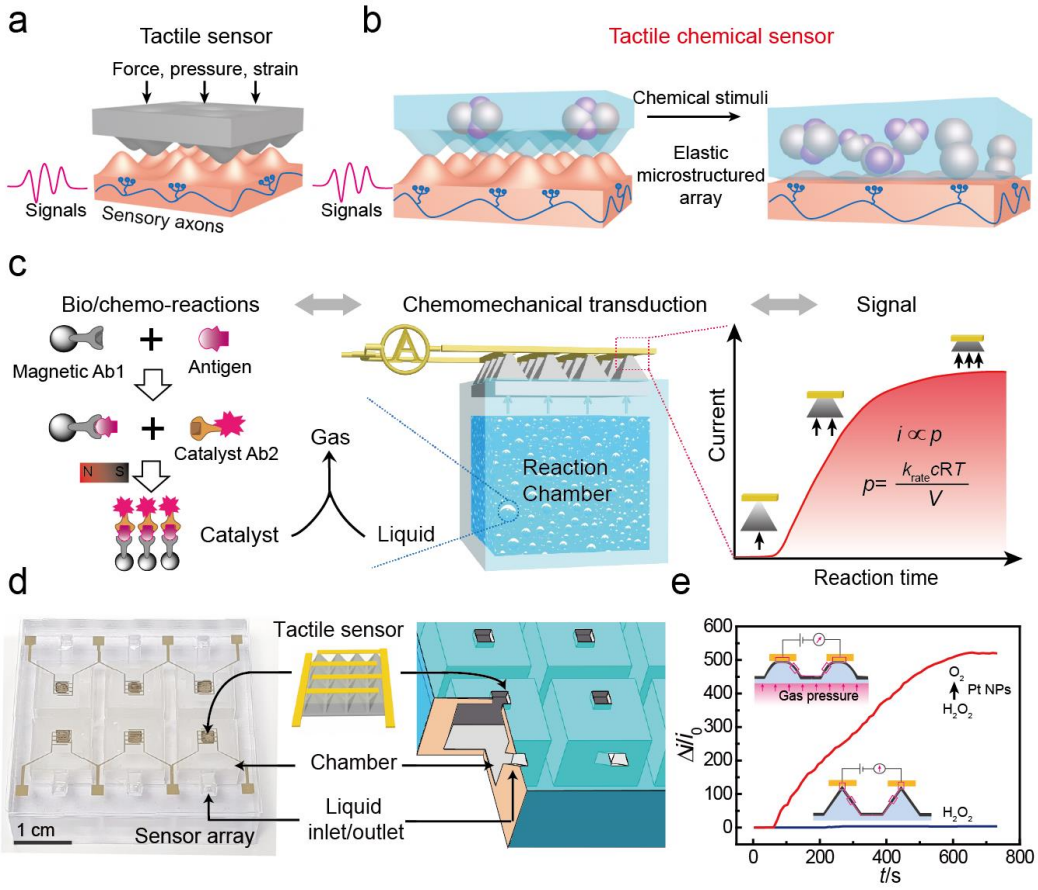

Figure 1. Scheme of tactile chemomechanical transduction for portable biosensing. a) Current tactile sensors for monitoring physical signals. b) Concept of tactile chemomechanical transduction based on elastic microstructured array for monitoring chemical signals. c) The principles for tactile biosensor. The design comprises of a biomarker-induced gas-producing reaction and a pyramidal tactile sensor. Tactile sensor based on elastic pyramidal array is expected to quantitatively transfer the concentration of biomarker to current signals, as described by the equation, where i is the current, p is the pressure, c is the concentration, T is the temperature, k_{rate} is the decomposition rate, and R is the ideal gas constant. d) The digital image of 3D-printed device array and their cross-section view. Each device contains a reaction chamber and two channels. e) Real-time readout of the catalytic decomposition of H_2O_2 by tactile chemomechanical device.

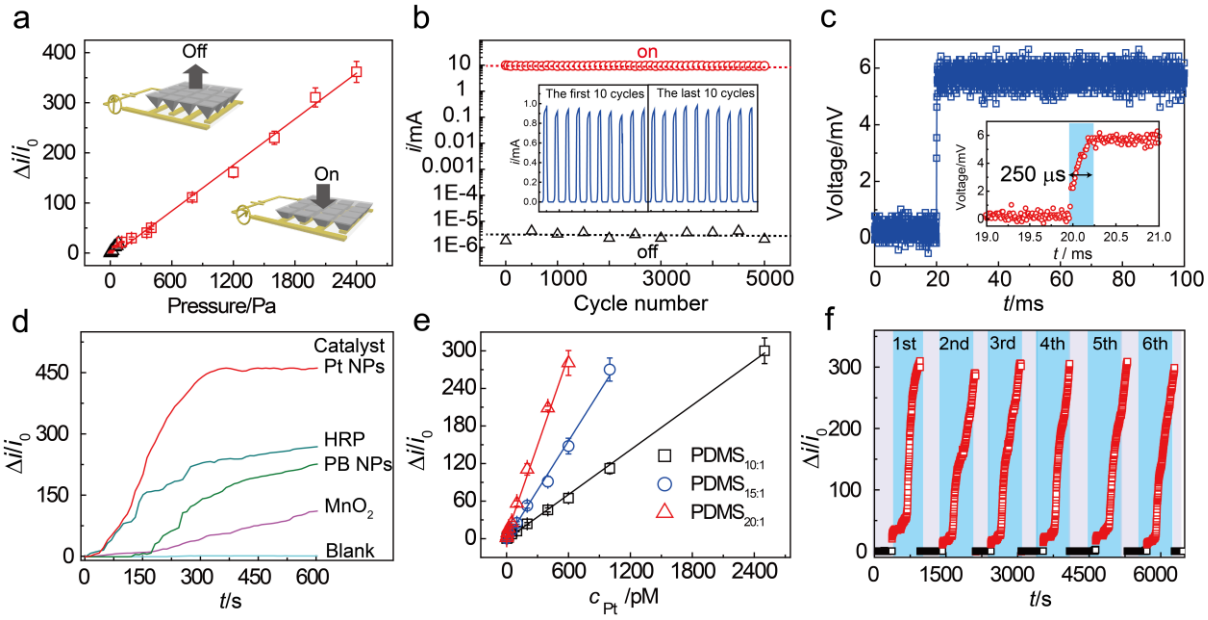

Figure 2. Characterization of the chemomechanical transduction capacity of tactile sensors. a) The linear response of pyramidal tactile sensors to pressure. b) Stability of the sensor is demonstrated by applying and releasing pressure of 2000 Pa for 5000 cycles. c) Response time of the tactile sensor to pressure (250 μs). The inset shows the magnification of voltage changing area. d) Tactile sensors for monitoring the catalytic decomposition of H_2O_2. H_2O_2: 1 M; catalysts (Pt NPs, HRP, PB NPs, MnO_2): 5 nM. The largest current increment indicates the highest catalytic efficiency of Pt NPs. e) Tunable linear detection range of Pt NPs by tactile sensors. Pyramidal $PDMS_{10}$, $PDMS_{15}$, and $PDMS_{20}$ with decreasing Young's modulus in sequence show an increase of chemomechanical transducing sensitivity. f) The stable cycling performance of tactile sensors for continuing monitoring the catalytic decomposition of H_2O_2.

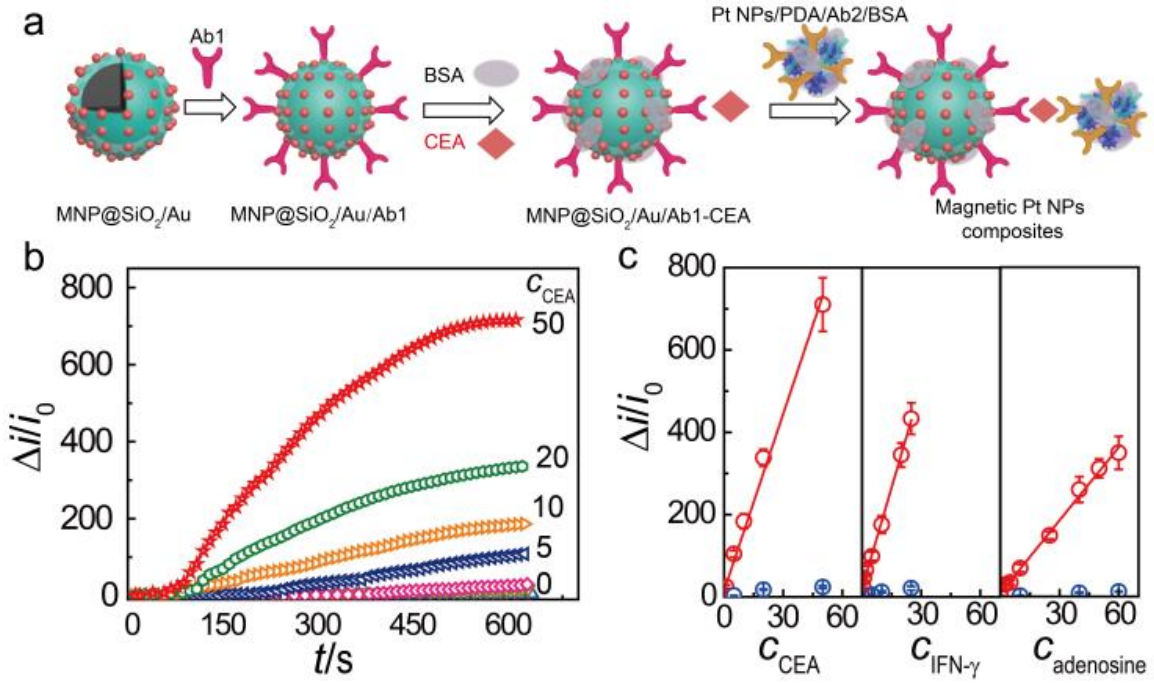

Figure 3. Sensing performance of tactile biosensors for various biomarkers. a) Schematic illustration of CEA immunoassay based on magnetic particles for separation and Pt NPs as labels. b) The current response of tactile biosensors for CEA with concentrations from 0 to 50 ng/mL. c) The linear detection of tactile biosensors for CEA (ng/mL), IFN-γ (nM), and adenosine (μM), respectively.

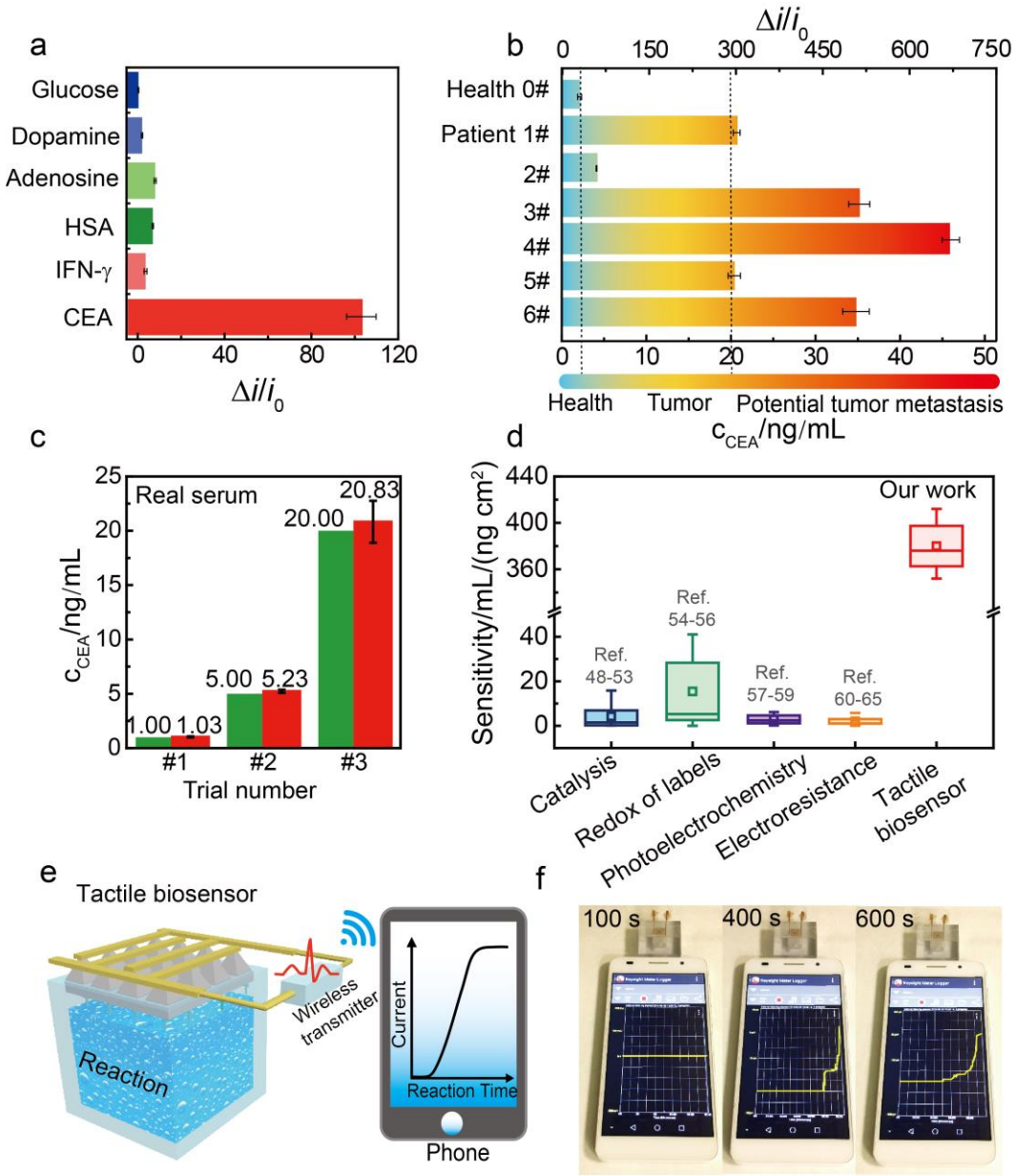

Figure 4. Evaluation of the tactile chemomechanical transduction for portable biosensing. a) Selectivity of tactile biosensors for CEA. Tactile biosensors for CEA detection using b) clinic serum samples and c) serum samples spiked with CEA. d) Performance comparison of tactile biosensors with current electrical transduction methods. Tactile chemomechanical transduction enhanced the sensitivity by 10-fold based on a triple-step amplification strategy. The configuration e) and photo images f) of tactile biosensors integrated with wireless technology for portable CEA biosensors. The photo images are collected at reaction interval of 100, 400 and 600 s.

The table of contents entry

Tactile chemomechanical transduction is proposed which allows tactile sensors to perceive bio/chemical signals. Based on elastic pyramidal array, tactile sensors transduce chemical signals from biomarker-induced gas-producing reactions to electrical signals. This concept broadens the application domain of tactile sensor and also provides a general and ultrasensitive transduction principle for portable biosensors.

Tactile sensor, chemomechanical transduction, healthcare, microstructured array, signal amplification

Ting Wang, Dianpeng Qi, Hui Yang, Zhiyuan Liu, Ming Wang, Wan Ru Leow, Geng Chen, Jiancan Yu, Ke He, Hongwei Cheng, Yun-Long Wu, Han Zhang,* and Xiaodong Chen*

Tactile Chemomechanical Transduction Based on Elastic Microstructured Array to Enhance the Sensitivity of Portable Biosensors